2023 IEEE 3rd International Conference on Sustainable Energy and Future Electric Transportation (SEFET) | 979-8-3503-1997-2/23/$31.00 ©2023 IEEE | DOI: 10.1109/SEFET57834.2023.10244965

Data-Centric Decentralised Controller for effective P-f and Q-V control in AC Microgrids

[a] Sheikh Mohammad Tayyeb, [b]Ram Krishan, Member IEEE
Department of Electric Engineering
National Institute of Technology Warangal, India
[a]stee21301@student.nitw.ac.in, [b]rkrishan@nitw.ac.in

***Abstract*—Accurate sharing of active and reactive powers in AC microgrids is one of the challenging problems. Implementation of Artificial Intelligence (AI) techniques seems to be a promising solution to enhance the control and operation of microgrids. This paper presents a novel method of data-centric AI-based decentralized frequency (f) and voltage (V) controller while sharing the proportional active and reactive power among the distributed generation (DG) units in the microgrids. In the proposed decentralized controller a Multi-Output Regressor based AI model is used for faster control action with accuracy. Once the controller model is trained, validated and tested on the microgrid data set for benchmark accuracy, it can be effectively used in real-time operation. The effectiveness of the proposed controller has been demonstrated on a Voltage Source Converter (VSC) based microgrid and compared with the traditional droop controller under various loading conditions.**

***Index Terms*—Multi-Output Regressor, Artificial Intelligence, inner current controller, outer voltage controller, AC microgrid**

I. Introduction

Microgrid is a flexible and reliable network having a group of interconnected loads and Distributed Generations (DGs) of electricity. It can be operated in both, islanded and grid-connected modes. Generally, the main source of power supply in microgrids is renewable energy sources (RES). However, large-scale RES in a system leads to various operating challenges [1]. Various problems related to grid integration of inverter-based resources (IBRs) including solar, wind and battery energy resources have been proposed in [2]-[3]. Frequency and voltage control of the microgrid having large-scale integration of IBRs are very essential. In such types of microgrid systems, the dynamics of voltage source converter (VSC) study and tuning of gains of conventional droop controllers are critical aspects in the real-time operation.

An overview of various technical control solutions at different levels of microgrid organization hierarchy has been analysed in [4]. Advancement in power converter topology and control strategies has led to better reliability, conversion efficiency and grid resiliency [5]. As per current loading conditions, droop-based control generates the reference frequency and voltage for inverter operation. In the controller, the outer voltage controller maintains the bus voltage while the inner current loop prevents the converter switches from overcurrents. Conventionally, proportional-integral (PI) controllers are suited for this operation. Different classical controllers like PI, PID, Lead, lag, etc compensators have been analysed in [6]. A comparison of the performance of various controllers like fuzzy logic proportional-integral (FPI) controller, PI controller and the model predictive control (MPC) for frequency regulation of isolated microgrid is given in [7]. In PI controllers, frequent tuning of various gains is very challenging, especially in new operating conditions. Also, too many PI controllers possess a problem of lag in controller response [8]. A decentralised MPC scheme is employed in [9] for voltage regulation at the point of common coupling in islanded DC microgrids. The main drawback of MPC is that the optimal control problem is to be solved online and under real-time constraints. There are various hierarchical control methods developed for the microgrids such as Primary, secondary and tertiary controls. Their drawbacks and an extensive study on the possibility of AI implementation in different control layers are given in [10].

The authors in [11] had discussed the combination of traditional methods and AI-based approaches as a promising tool for microgrid control in response to stochastic system dynamics and stability requirements. Also, it has been mentioned that explicit system models are not needed, and control stability can be ensured.

From the above literature review, there are very few AI-based controllers available for AC microgrids [13]. However, the available AI-based controllers are lacking in efficient design and faster operation. Further, the conventional PI-based droop controllers demand the proper tuning of gain parameters and constants for effective power sharing in microgrids which is very complex. Therefore in this paper, a data-centric AI (DCAI) method is proposed for designing a microgrid controller with a faster and better response. The important features of the proposed method are as follows: This controller design is based on Multi-Output Regressor (MOR) analysis [12] in which output is just the linear combination of weighted input features.

- Design of data-centric AI-based decentralized controller for frequency and voltage control of AC microgrid.
- Unlike the neural network [13] based controller, the proposed controller is based on a multi-output regression

This research was supported by Science and Engineering Research Board (SERB) DST India under grant number SRG/2021/000810.

979-8-3503-1997-2/23/$31.00 ©2023 IEEE

method and it is used to achieve an accurate and faster response.
- The proposed DCAI method shows robust performance in comparison with conventional closed-loop PI controllers.

The remaining paper is organised as follows. In Section II, modelling of the basic controller is given. The multi-output regression method is described in Section III. Section IV describes the simulation, results and its discussion for a given test system and comparison with the neural network model. Finally, the conclusion of the paper is given in Section V.

II. VSC Controller Modeling

The AC microgrid may consist of various IBRs and loads connected through distribution lines. In AC microgrids Voltage source converters (VSCs) are connected in parallel and their controller consists of an outer voltage controller and an inner current controller. In such arrangements, droop-based references are provided which originate from the principle of power balance in synchronous generators. The difference between the input mechanical power and the output electric power causes a change in the rotor speed and hence system frequency. Similarly, variation in output reactive power results in voltage magnitude deviation. Such a characteristic can be artificially created for electronically interfaced inverter-based AC microgrid [14]. In droop control, the relationships between real power (P) and frequency (ω) and reactive power (Q) and voltage (V) are as follows:

$$\omega_{ref} = \omega_{nominal} - m_p * P \tag{1}$$

$$v_{ref} = v_{nominal} - n_q * Q \tag{2}$$

where m_p and n_q are droop constants.
The differential equation for the outer voltage controller is derived from filter capacitor (C_f) as:

$$C_f \frac{\partial v_{od}}{\partial t} = i_{fd} - i_{od} + \omega_o * C_f * V_{oq} \tag{3}$$

$$C_f \frac{\partial v_{oq}}{\partial t} = i_{fq} - i_{oq} - \omega_o * C_f * V_{od} \tag{4}$$

where v_{od} , v_{oq} ,i_{od} and i_{oq} are output voltage and current in dq frame.
Optimal gain and phase margin analysis can be used for calculating the proportional and integral constants of outer voltage controller i.e. Phase margin may be kept between 30^o and 70^o.

$$K_{pv} = C_f * \omega_{gc} \tag{5}$$

$$K_{iv} = K_{pv}/\tau_v \tag{6}$$

where ω_{gc} is gain cross-over frequency and τ_v is time constant for outer voltage controller.
Similarly, mathematical model for the inner current controller can be derived from RL branch dynamics as:

$$L_f \frac{\partial i_{fd}}{\partial t} = V_{fd} - V_{od} + \omega_o * L_f * i_{fq} - R_f * i_{fd} \tag{7}$$

$$L_f \frac{\partial i_{fq}}{\partial t} = V_{fq} - V_{oq} - \omega_o * L_f * i_{fd} - R_f * i_{fq} \tag{8}$$

The proportional and integral constants of PI control in inner current controller are chosen such that pole-zero cancellation occurs to improve the stability. It can be described as-

$$K_{ic} = R/\tau_c \tag{9}$$

$$K_{pc} = L/\tau_c \tag{10}$$

where τ_c is time constant for inner current controller.
The above PI constants K_p and K_i need to be finely tuned for proper control operation. It is not required in AI-based controllers, it can be directly deployed once the model, is trained and validated with standard data.

III. Multi-Output regression

A. Definition

Multi-output regression (MOR) consists of fitting one regressor per target. The relationship between outputs and inputs can be realised using input data and output data points. In this paper, we are using the MOR with estimator Ridge: Linear least squares with L_2 regularization. This model solves a regression model where the loss function is the linear least squares function and regularization is given by the L_2 norm also known as Ridge Regression or Tikhonov regularization. The regression equation in this machine-learning model can be written as:

$$\mathbf{Y = WX + e} \tag{11}$$

Where Y and X is representing the dependent and independent variables respectively. W is the regression coefficient to be estimated and e represents the error residuals.

B. Cost function

The cost function used for ridge regression is :

$$min(||Y_{actual} - wX||^2 + \lambda||w||^2) \tag{12}$$

where λ is the penalty term. So, the penalty term can be controlled by changing the values of λ. For higher values of λ, the penalty will be high and therefore the magnitude of coefficients is reduced. Advantages of using λ are:
- It shrinks the parameters. Therefore, it is used to prevent multicollinearity.
- It reduces the model complexity by coefficient shrinkage so as to prevent the model from over-fitting.

The mathematical equations derived after training the multi output regressor model is given in (13) and (14) with coefficients of m_d and m_q after training given in Table IV

$$\begin{aligned} m_d = {} & w_1 I_{fd} + w_2 I_{fq} + w_3 I_{od} + w_4 I_{oq} \\ & + w_5 V_{od} + w_6 V_{oq} + w_7 W + b \end{aligned} \tag{13}$$

$$\begin{aligned} m_q = {} & w_1 I_{fd} + w_2 I_{fq} + w_3 I_{od} + w_4 I_{oq} \\ & + w_5 V_{od} + w_6 V_{oq} + w_7 W + b \end{aligned} \tag{14}$$

where m_d and m_q are modulating signals and these signals are input to abc/dqo converter as depicted in Fig. 2.

C. Steps in Multi-output-Regressor

1) Load the dataset into the pandas data frame object. The dataset is generated from the model given in Fig.**??**
2) Normalize the data frame object.
3) Split the data into training and testing data.
4) Form the model using Multi-output Regressor with Ridge as the estimator.
   $model = MultiOutputRegressor($
   $Ridge(randomstate = 123))$
   The $randomstate$ hyperparameter is used to control any such randomness involved in machine learning models to get consistent results.
5) Fit the training data and predict the testing data.
   $model.fit(X_{train}, Y_{train})$
   $model.predict(X_{test})$
6) Model is evaluated based on model score and mean squared error. Model score is given by:

$$Model\ score = \frac{\sum (Y_{test} - Y_{pred})^2}{\sum (Y_{test} - Y_{test,mean})^2}$$

Model score is a statistical measure of how well the regression predictions approximate the real data points.

IV. Results and Discussion

A. Test System

The test system consists of an AC microgrid with two VSCs feeding multiple loads. The reference frequency and voltage are generated by droop control while the outer-voltage controller maintains the bus voltage and the inner current loop prevents the converter from over-currents. The design of voltage and the current controller is based on dynamics equations in dq reference frame as given in (3),(4),(7) and (8)

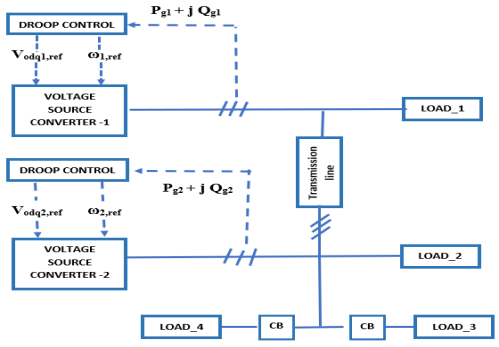

Fig. 1. Block diagram of AC microgrid.

The block diagram of the AC microgrid is given in Fig. 1. Similar to the traditional PI controller, a VSC with MOR based controller is shown in Fig. 2. The VSC parameters with LCR filter are given in Table I. The LCR filter values are calculated as mentioned in [15]. As the sampling frequency is 50 KHz, the switching frequency is kept at 1 KHz so that 50 data points are generated in one switching cycle. For the result comparison PI controller parameters K_p and K_i can be

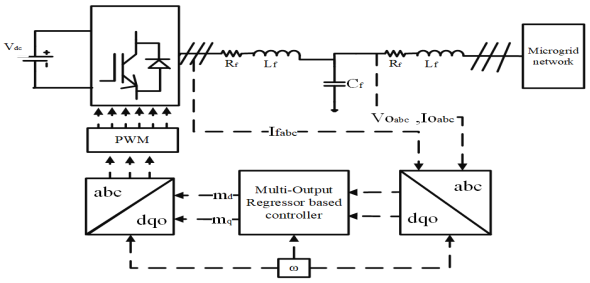

Fig. 2. VSC with Multi-Output Regressor controller

calculated using eq (5), (6),(9) and (10) and given in Table-II.

TABLE I
Model Parameters

VSC parameters			
$f_{sw} = 1$ KHz	$V_{dc} = 700$ V	$T_s = 20\ \mu sec$	$R_f = 0.1\ \Omega$
$L_f = 3.5$ mH	$C_f = 50\mu F$	$\tau_c = 63.66\ \mu sec$	$\tau_v = 480.56\ \mu sec$
$m_p = 0.00005$	$n_q = 0.003$	$\omega_{gc} = 1/sqrt(\tau_c * \tau_v)$ = 5717.33 rad/sec	
Transmission and load parameters			
Transmission Line		$L_c = 0.35$ mH	$R_c = 0.15\ \Omega$
$Load_1 = load_2$		$P = 1000$ watt	$Q = 200$ VAR
$Load_3$		$P = 3000$ watt	$Q = 200$ VAR
$Load_4$		$P = 2000$ watt	$Q = 200$ VAR

T_s: sampling time (50 data points in one switching cycle)

TABLE II
Controller Parameters

Outer voltage controller	$K_{pv} = 0.2859$	$K_{iv} = 594.8499$
Inner current controller	$K_{pc} = 54.9779$	$K_{ic} = 1570.8$

B. Simulation Results

$load_1$ and $load_2$ (P = 1000 watt, Q = 200 VAR) are connected throughout simulation run. Additional, three phase load , $load_3$ with P = 3000 watt, Q = 200 VAR is connected to bus_2 at time $t = 1\ sec$ and disconnected at $t = 3\ sec$. Similarly, $load_4$ with P= 2000 watt, Q= 200 VAR is connected to bus_2 at time $t = 2\ sec$ and disconnected at $t = 3\ sec$. Various waveforms for above loading conditions with same droop slope m_p and n_q are given below.

- There is no large dip in voltage when different loads are connected and controller is able to maintain the output voltage of VSC around 220 V (rms) as shown in Fig.3. The three phase output voltage is pure sinusoidal in nature as depicted in Fig.4. The change in loading has negligible effect on output voltage.

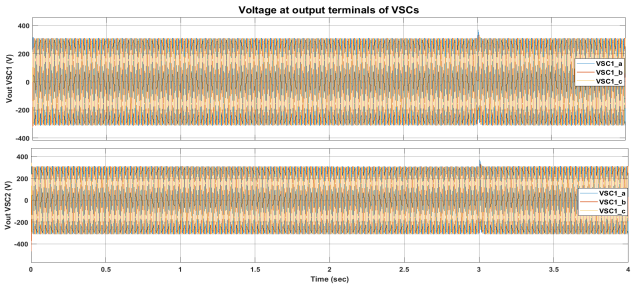

Fig. 3. Voltage at output terminals of VSCs.

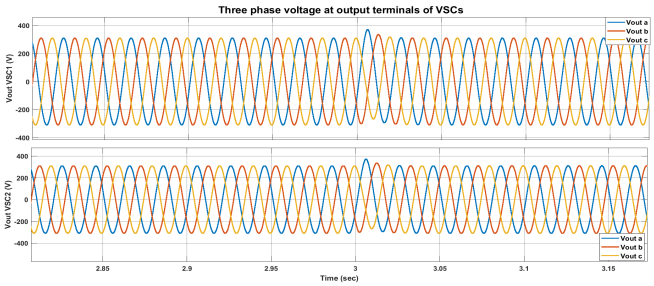

Fig. 4. Voltage at output terminals of VSCs (zoom-in time-axis).

- The current at output terminals of VSC_1 and VSC_2 is depicted in Fig. 5 and Fig. 6. The effect of additional $load_3$ and $load_4$ at time $t = 1\ sec$ and $t = 2\ sec$ respectively and disconnection of both $load_3$ and $load_4$ at time $t = 3\ sec$ is illustrated with the current waveforms as shown in in Fig. 5 and Fig. 6.

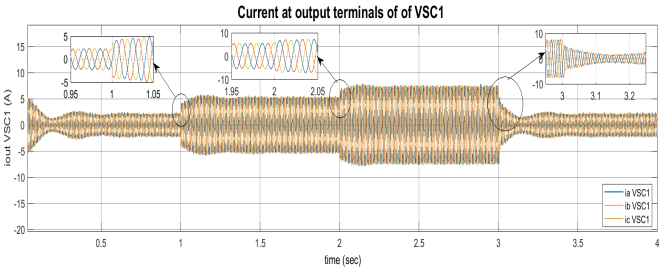

Fig. 5. Current at output terminals of VSC1.

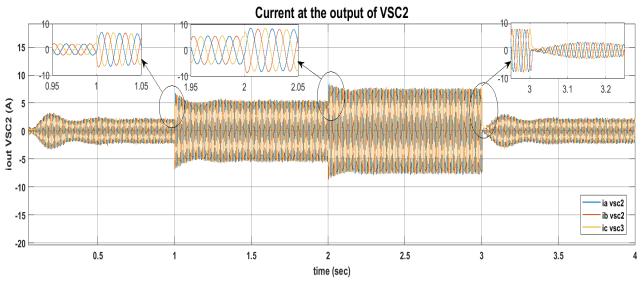

Fig. 6. Current at output terminals of VSC2 .

- The P-f and Q-v waveforms are illustrated in Fig. 7 and Fig. 8. Equal active power sharing is ensured due to frequency being a global phenomenon while reactive power sharing is proportional in nature due to voltage being a local phenomenon.

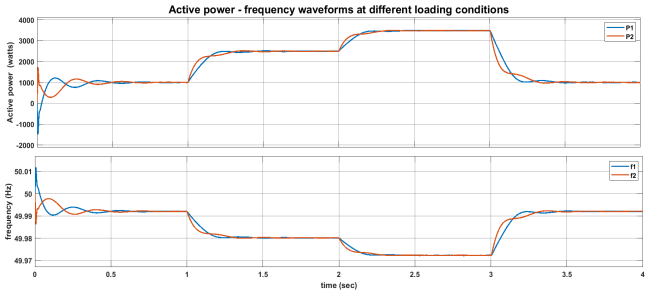

Fig. 7. Power-Frequency waveforms under different loading conditions.

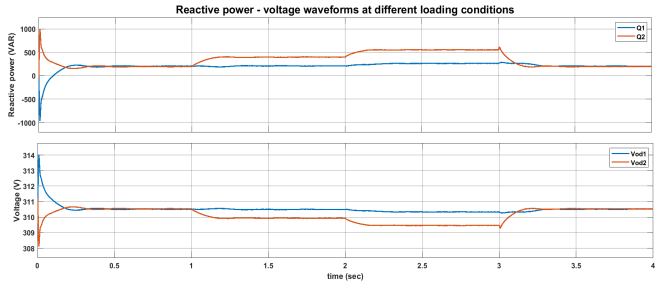

Fig. 8. Reactive power and Voltage waveforms under different loading conditions.

- **Comparison with the neural network:** Comparison of active power with the Multi-Output regressor model and neural network model with the same loading conditions is shown in Fig. 9. Large transients can be seen in the neural network model initially as depicted in Fig. 10.

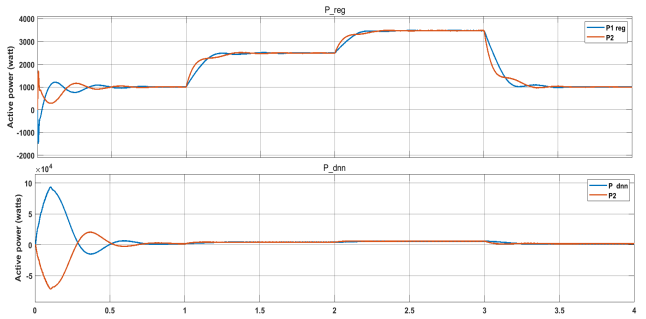

Fig. 9. Active power waveforms for Multi-Output regressor model and neural network model under different loading conditions.

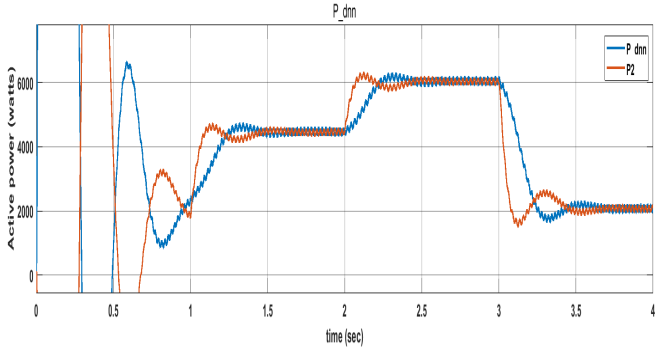

Fig. 10. Active power waveforms neural network model under different loading conditions (zoomed in along y axis).

Similarly, a comparison of reactive power with proposed model and neural network model with the same loading conditions is shown in Fig. 11. Proportional reactive power sharing is observed in MOR model while large deviation in reactive power sharing is observed in neural network based model.

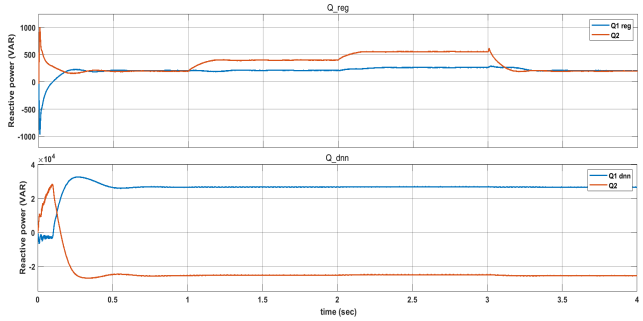

Fig. 11. Reactive power waveforms for the proposed model and neural network model under different loading conditions.

- For modelling the controller based on MOR, the steps given in section III-C are followed. The dataset is normalised and illustrated by histogram in Fig. 12. Different spikes in the graph represent changes in loading conditions (addition of loads at different time stamps). Therefore data points corresponding to that change are shown by spikes in the histogram.
  The neural network model consists of three layers with 16 neurons, 8 neurons and 2 output neurons respectively. The neural network is also trained on the same normalised dataset.
  The data is split in the ratio of 90% training data and 10% testing data as given in Table III. Both the models are trained on training data and validated on test data and comparison is done based on model score.

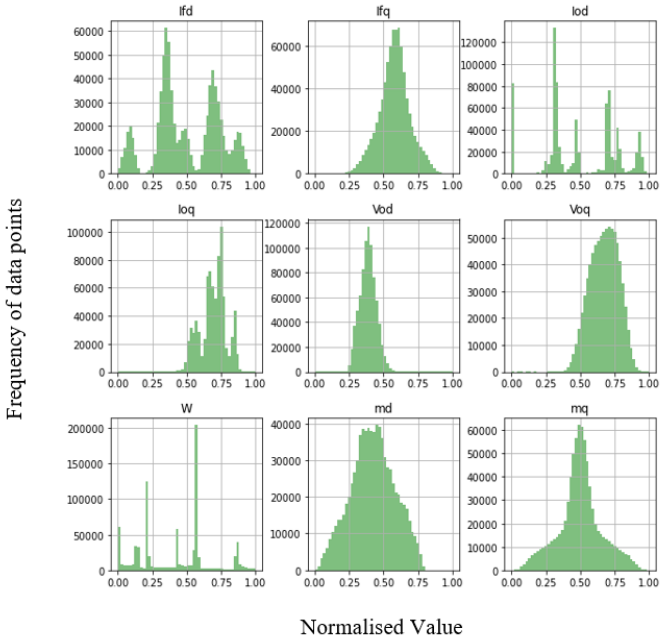

Fig. 12. Histogram of normalised data set

TABLE III
TRAINING AND TEST DATA

	rows	columns
X_{train}	720751	7
Y_{train}	720751	2
X_{test}	78751	7
Y_{test}	78751	2

The mean squared error and model score for model evaluation is given in Table IV. A model score of 1 indicates that the regression predictions perfectly fit the data. The coefficients of m_d and m_q for MOR model are given in Table V

TABLE IV
MODEL EVALUATION

	Mean squared error	Model score
Multi Output Regressor model	7.0264*10−5	0.99719
Neural network model	0.2045	-2.862

C. Discussion

The model_score of 0.99719 and Mean squared error of $7.0264 * 10^{-5}$ signifies that the model is fitting the test data well. Therefore the predictions of our proposed model ($Y_{predictions}$) are identical to the output values (Y_{test}) of PI based VSC controller. Unlike PI controllers, the proposed MOR based VSC controller has faster response as there are

TABLE V
COEFFICIENTS OF m_d AND m_q FOR MORMODEL

	m_d coefficients	m_q coefficients
w_1	-4.9734	0.1071
w_2	-0.0292	-1.5551
w_3	4.3729	-0.0056
w_4	0.0657	0.7013
w_5	-0.4480	0.0827
w_6	-0.0231	-0.1612
w_7	0.1477	-0.0039
b	0.8491	0.9409

no inner and outer control loops. It can be used for any real time application in microgrids. The $Y_{predictions}$ and Y_{test} have been taken from random samples of the test data analysis for comparison of the responses of the test system with output of the PI controller (Y_{test}) and predicted output from Multi-Output Regressor ($Y_{predictions}$) and predicted output from neural network model. The values of modulating signals m_d and m_q obtained using these different control strategies are given in Table-VI.

TABLE VI
COMPARISON OF MODULATING SIGNALS OBTAINED WITH MULTI OUTPUT REGRESSOR MODEL (MOR), NEURAL NETWORK MODEL AND PI MODEL BASED CONTROLLERS

Y_{test} $(PI\ controller)$			$Y_{predictions}$ $(MOR\ model)$		$Y_{predictions}$ $(NN\ model)$	
S no.	m_d	m_q	m_d	m_q	m_d	m_q
1	0.1490	0.5377	0.1542	0.5383	0.1299	0.5910
2	0.3252	0.8131	0.3281	0.8176	0.0448	0.3874
3	0.3623	0.5772	0.3559	0.5791	0.1748	0.6911
4	0.0939	0.4165	0.0929	0.4204	0.2266	0.8640
5	0.6145	0.5243	0.6169	0.5158	0.1451	0.6578
6	0.4248	0.4698	0.4272	0.4647	0.1580	0.7102
7	0.2766	0.4878	0.3022	0.4959	0.1291	0.5690
8	0.5179	0.5941	0.5111	0.5946	0.1007	0.5378
9	0.3812	0.4457	0.3862	0.4388	0.2076	0.7981
10	0.4344	0.4418	0.4490	0.4499	0.2110	0.8102

V. CONCLUSION

In this paper, a novel AI control strategy based on the Multi-output-Regressor model has been proposed for the DG connected through VSC in an AC microgrid. First, data preprocessing has been done to obtain a reliable data set for the training of the AI controller and further, it is deployed in a microgrid test system having two VSC for validation. The simulation results were compared with the conventional PI and neural network model-based droop controller. The model evaluation metrics signify that the MOR model has fitted well with data and the mean squared error is very less i.e. $7.0264 * 10^{-5}$. Hence, the proposed model can be used to replace the conventional PI-based Inner current controller and outer voltage controller to achieve a faster control operation without tuning any controller parameters. Also, a neural network is computationally expensive with a lot of parameters to be learned while in the proposed MOR model, the coefficients to learn are small.

The future scope lies in testing it for different microgrid architectures and its implementation in hardware systems.

REFERENCES

[1] Badal, F.R., Das, P., Sarker, S.K. et al. A survey on control issues in renewable energy integration and microgrid. Prot Control Mod Power Syst 4, 8 (2019).

[2] M. Shafiullah, S. D. Ahmed and F. A. Al-Sulaiman, "Grid Integration Challenges and Solution Strategies for Solar PV Systems: A Review," in IEEE Access, vol. 10, pp. 52233-52257, 2022.

[3] M. H. Saeed, W. Fangzong, B. A. Kalwar and S. Iqbal, "A Review on Microgrids' Challenges & Perspectives," in IEEE Access, vol. 9, pp. 166502-166517, 2021.

[4] 2. Z. Tang, Y. Yang and F. Blaabjerg, "Power electronics: The enabling technology for renewable energy integration," in CSEE Journal of Power and Energy Systems, vol. 8, no. 1, pp. 39-52, Jan. 2022

[5] A. Vasilakis, I. Zafeiratou, D. T. Lagos and N. D. Hatziargyriou, "The Evolution of Research in Microgrids Control," in IEEE Open Access Journal of Power and Energy, vol. 7, pp. 331-343, 2020.

[6] V. Gurugubelli, A. Ghosh and A. K. Panda,"Droop controlled voltage source converter with different classical controllers in voltage control loop," 2022 IEEE International Conference on Power Electronics, Smart Grid, and Renewable Energy (PESGRE), 2022, pp. 1-6.

[7] M. U. Jan, A. Xin, H. U. Rehman, M. A. Abdelbaky, S. Iqbal and M. Aurangzeb, "Frequency Regulation of an Isolated Microgrid With Electric Vehicles and Energy Storage System Integration Using Adaptive and Model Predictive Controllers," in IEEE Access, vol. 9, pp. 14958-14970, 2021.

[8] M. Abbasi, N. M. Dehkordi and N. Sadati, "Decentralized Model Predictive Voltage Control of Islanded DC Microgrids," 2020 11th Power Electronics, Drive Systems, and Technologies Conference (PEDSTC), 2020, pp. 1-6.

[9] T. Sreekumar and K. S. Jiji, "Comparison of Proportional-Integral (P-I) and Integral-Proportional (I-P) controllers for speed control in vector controlled induction Motor drive," 2012 2nd International Conference on Power, Control and Embedded Systems, 2012, pp. 1-6.

[10] Rohit Trivedi, Shafi Khadem,"Implementation of artificial intelligence techniques in microgrid control environment: Current progress and future scopes,"Energy and AI,Volume 8,2022,100147,ISSN 2666-5468.

[11] Tao Wu, Jianhui Wang,"Artificial intelligence for operation and control: The case of microgrids",The Electricity Journal,Volume 34, Issue 1,2021,106890,ISSN 1040-6190.

[12] Jin Wang, Zhiliang Chen, Kaiwei Sun, Hang Li, Xin Deng,"Multi-target regression via target specific features",Knowledge-Based Systems,Volume 170,2019,Pages 70-78,ISSN 0950-7051.

[13] LeCun, Y., Bengio, Y. and Hinton, G. Deep learning. Nature 521, 436–444 (2015).

[14] M. Ramezani and S. Li, "Voltage and frequency control of islanded microgrid based on combined direct current vector control and droop control," 2016 IEEE Power and Energy Society General Meeting (PESGM), 2016, pp. 1-5.

[15] M. Dursun and M. K. DÖŞOĞLU, "LCL Filter Design for Grid Connected Three-Phase Inverter," 2018 2nd International Symposium on Multidisciplinary Studies and Innovative Technologies (ISMSIT), Ankara, Turkey, 2018, pp. 1-4.